Effects of scattering due to seafloor microrelief on a multifrequency sonar seabed profiler

Bishwajit Chakraborty
National Institute of Oceanography, Dona Paula, Goa 403 004, India

(Received 21 June 1988; accepted for publication 9 November 1988)

A theoretical study of the interaction effect of circular beams generated by coaxial circular array operated at useful frequencies with different beam widths is carried out for different types of seabed ripples. Analysis, by means of calculation of the probability density function (PDF) of the echo amplitude, echo waveform structure, and reflected echo energy density, shows that the fluctuation effects are prominent even at the most narrow beam width at an operating frequency of 20 kHz for rippled bottoms of different sediment type. In this article, the operating frequencies and ripple parameters are more responsive toward scattering effects than narrow beam widths, generated by the coaxial circular array.

PACS numbers: 43.30 Hw, 43.30.Gv, 43.30.Vh

INTRODUCTION

Sonar reflection profiling of the seafloor is a routine method for various objectives, such as geological surveys to characterize the seabed, geotechnical properties, etc. In the past few years, a considerable amount of work was undertaken to develop acoustic signal processing techniques to determine the quantitative as well as qualitative distinction between bottom characteristics. The present work is devoted to the determination of the interaction effects of the three rippled sea bottoms of different sediment type (sand, silt, and clays of specific ripple heights and wavelengths) with the circular sonar beams generated by our coaxial circular sonar array.[1] The array operable at five frequencies (60, 30, 20, 12, and 4 kHz), is chosen for this current study because the scattering effects are frequency dependent. The sonar's beam patterns are summarized in Table I.

In order to classify the seabed, the interaction effect of the bottom relief on an acoustical signal must be known. Stanton and Clay,[2] Dunsiger *et al.*,[3] and many workers,[4,5] have done some amount of work to identify the bottom type from its reflection and scattering characteristics. For example, Stanton[4] demonstrated that the probability density function (PDF) of the echo amplitude depended on the seafloor roughness, sonar beam width, and frequency—especially at lower frequencies where the wavelength of sound is much greater than the root-mean-square (rms) roughness of the floor. Based upon that work, PDFs were calculated at lower frequencies like 20, 12, and 4 kHz by our coaxial circular array for different types of rippled bottom. To satisfy the criterion to employ the Helmholtz–Kirchhoff condition ($4k^2\Omega^2 \ll 1$), where k is the operated wavenumber and Ω is the rms roughness of the sea bottom; the higher frequencies (30 and 60 kHz) are not considered. Previously published ripple height and wavelength parameters for different types of ripples, tabulated in Table II, are used for the present study.[3,6]

Determination of echo waveforms and related echo energy densities reflected from different sediments, along with the knowledge of PDF, are important tools to predict the type of bottom.[7] In view of that, waveforms of the reflected echoes are also presented for different pulse lengths (2.12 and 4.2 ms). In addition, study of calculated energy densities for different rippled seabeds are also carried out.

I. ANALYSIS

Figure 1 shows the geometry of the operating conditions of the array that is ship mounted. Since the beam widths depend upon operating frequencies, each beam insonifies a different area of the seabed. The maximum insonification area is obtained at the lowest frequency of 4 kHz. The sea bottom depth considered in present work is around 5000 m. The study involves only the echoes reflected back from water/bottom interface; i.e., penetration effects are not considered.

A. Echo fluctuations

Clay and Leong (in Stanton and Clay[2]) expressed the following relationship for correlation length of ripples in the form of their rms roughness:

$$I_x = 30\Omega^{1.25} \quad \text{(in m)}, \tag{1}$$

where I_x is the correlation length along the x axis. The correlation length along the y axis I_y is related to I_x by the following relationship:

$$I_y/I_x = \eta, \tag{2}$$

where η, depending on the ripple type, may vary from 1–5. In this study, η is chosen as 5; i.e., the ripple correlation length along the y axis is 5 times to the correlation length along the x axis. The Rice PDF describes the echo amplitude E from the seabed[2,8]:

TABLE I. Properties of the circular beam.

Sonar number	Frequency of operation in kHz	Half-power beam width of transceiver in degrees	Angle between the e^{-1} points of the transceiver (B) in degrees	Insonified radius in meters at the depth of 5000 m
1	4	26	40	1154.34
2	12	8.6	13	375.95
3	20	5.3	8	231.42

 0001-4966/89/041478-04$00.80

TABLE II. Properties of ripple mark considered in calculation.

Sonar number	Sediment type	rms ripple[a] roughness (height) in m	Correlation length in m		Corresponding ripple wavenumber (in m^{-1})		Density[b] (g/c c)	Sound velocity[b] (in m/s)
			along X	along Y	along X	along Y		
1	sand	0.011	0.1068	0.534	14.69	2.941	2.03	1836
2	clay	0.013	0.1316	0.658	11.92	2.387	1.42	1519
3	silt	0.015	0.1575	0.787	9.98	1.995	1.56	1522

[a] Adopted from Dunsiger *et al.*[3]
[b] Adopted from Bell and Porter.[6]

$$P(E) = [2E(1+G)/\langle E^2\rangle] \times \exp\{-[(1+G)E^2 + G\langle E^2\rangle]/\langle E^2\rangle\} I_0(Q), \quad (3)$$

where $I_0(Q)$ is the modified Bessel function and

$$Q = 2E[G(1+G)]^{0.5}/(\langle E^2\rangle)^{0.5}.$$

Here, $\langle E^2\rangle$ is the mean echo amplitude and G is the measure of the relative roughness or smoothness of the bottom and can be presented for a ripple bottom as[2]

$$G^{-1} = (300/\pi)B^2k^4\eta\Omega^{4.5}, \quad (4)$$

where B is the beam width between e^{-1} points in radians of the array beam pattern, k is the operating wavenumber, and Ω is the rms roughness, i.e., rms ripple height in the current study.

Figure 2 shows that the most narrow PDF is at the lowest operating frequency, 4 kHz for sand ripples. At the same frequency, the PDFs are broader for clay and silt due to higher rms roughness and, hence, more scattering. In general, the PDFs are Gaussian at the lowest frequency and become Rayleigh-like as the frequency increases. An increase in fluctuation, with frequency as well as roughness, is also supported by the calculated values of G with the help of Eq. (4), which is presented in Fig. 2. It can also be observed that the effect of narrow beams [B^2 in Eq. (4)] is dominated in the present observation, i.e., even at the most narrow beams (5.3°) at 20 kHz, by the fading effect due to roughness ($\Omega^{4.5}$) as well as frequency (k^4) of operation.

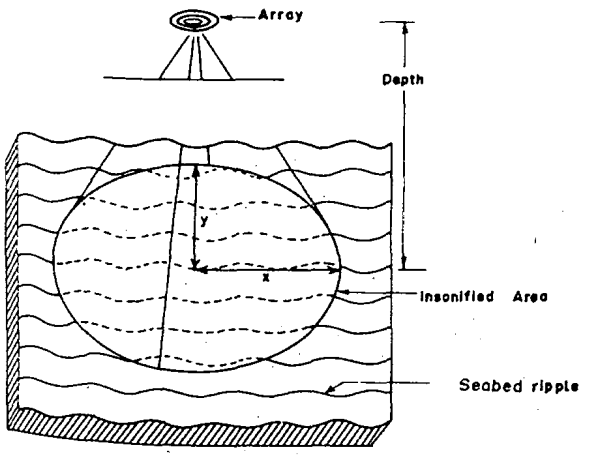

FIG. 1. Operating conditions of the coaxial circular array.

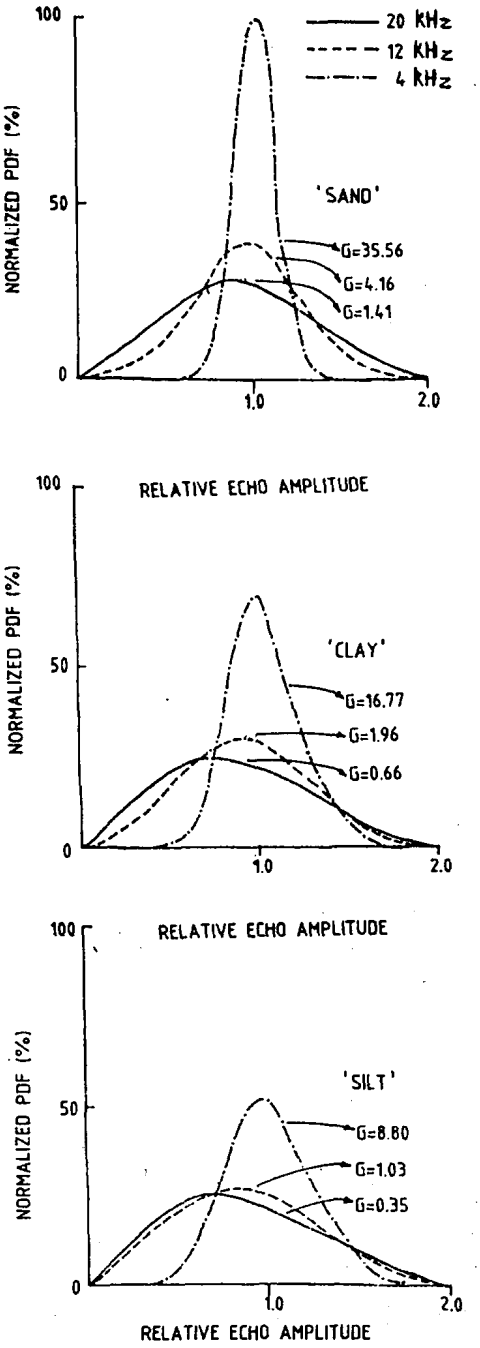

FIG. 2. PDF for different rippled sediment types.

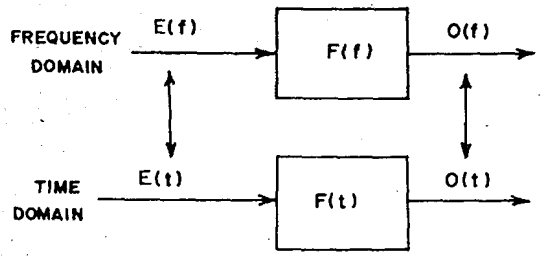

FIG. 3. Linear system approach towards diffraction problem.

B. Time decay of echoes

The corrugated bottom better suits our studies to predict the mean echo pattern for sonar performance in deeper water (5000 m) where current generated ripples (with rounded sawtooth relief[4]) are formed. Therefore, we assume that the ripple varies periodically along x axis and there is almost no variation along y axis, with this in Eq. (2), η can be chosen equal to 5. In order to predict the reflected waveform from such a bottom, we apply an expression from Tolstoy and Clay[9]:

$$E = \frac{ik\bar{B}xy}{r_1 r_2} Re^{-2\beta^2 Y^2} \cos\theta_1 J_0(2\gamma\Omega) e^{-2\alpha^2 X^2} + \sum_{n=1}^{\alpha} (i)^n f_1(\theta_1,\theta_n) J_n(2\gamma_n\Omega) e^{-(2\alpha_n - nK)^2 x^2/2} + \sum_{n=1}^{\alpha} (i)^n f_1(\theta_1,\theta_n) J_n(2\gamma_n\Omega) e^{-(2\alpha_n + nK)^2 x^2/2}, \quad (5)$$

where $k = 2\pi/\lambda$ and λ is the transmitted wavelength. However, a term $\bar{B}$ related to source power is considered to be unity. For circular insonification, x, y are distances along the X and Y axes; $x = y =$ the radius of the isonified area. For a coaxial circular array transducer, $r_1 = r_2$ at normal incidence. The plane-wave/plane-interface reflection coefficient is $R = (\rho_1 C_1 - \rho_2 C_2)/(\rho_1 C_1 + \rho_2 C_2)$, where $\rho_1 C_1$ is the product of density and velocity of the sediment material, respectively, and $\rho_2 C_2$ is the product of density and velocity of the water.

The term in the above expression shows that $f_1(\theta_1,\theta_n) = 1.0$ at the normal incidence direction, where $\theta_1 = 0°$, and θ_n is the diffraction angle. The vertical component, γ, of the reflected and the incident wavenumber is equal to $-k/2$,

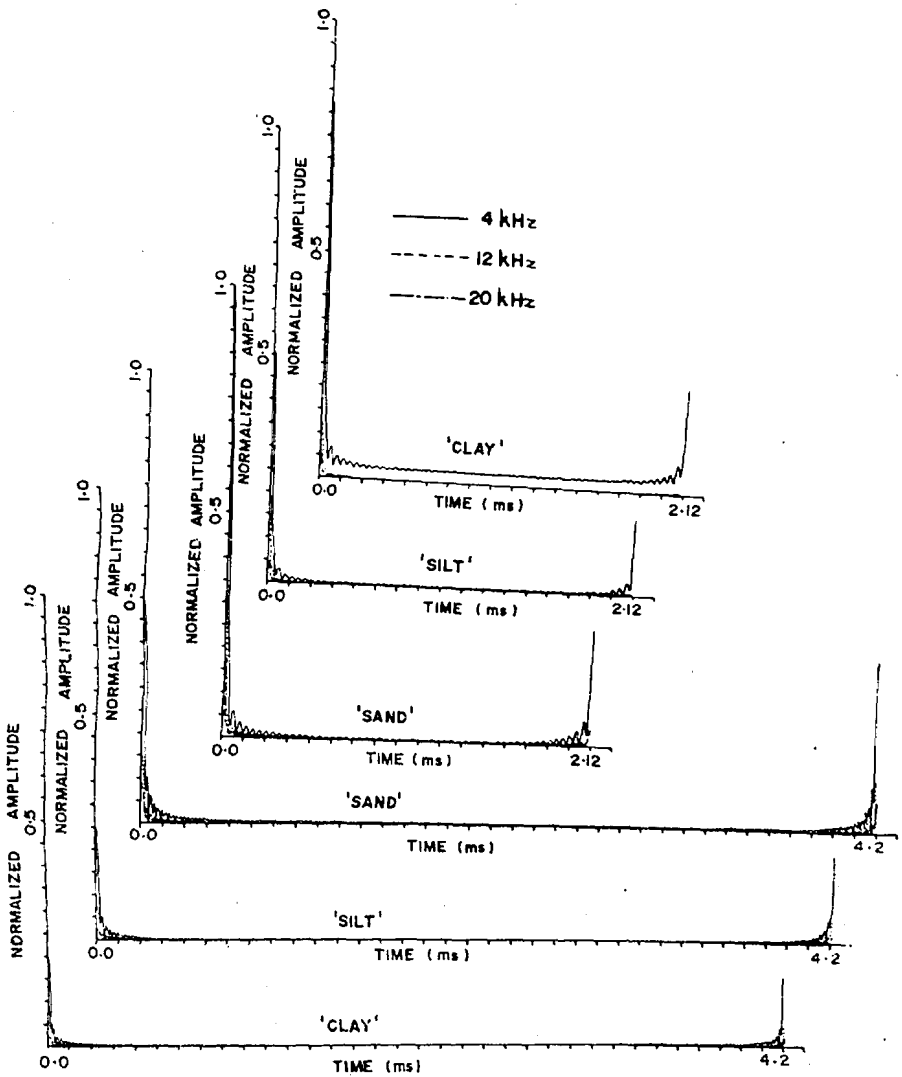

FIG. 4. Plot of $O(t)$ for different types of rippled bottom for pulse lengths of 2.12 and 4.2 ms.

and Ω is the rms ripple height. Similarly, other horizontal components of reflected wavenumbers are $\alpha = 0$ and $\beta = 0$ for vertical angles of incidence and reflection for the normal incident direction. Here, $J_0(2\gamma\Omega)$ is the zeroth-order Bessel function of argument $2\gamma\Omega$ and $J_n(2\gamma_n\Omega)$ is the nth-order Bessel function of $2\gamma_n\Omega$. Here, γ_n [$= k(1 + \cos\theta_{2n})$, θ_{2n} is the diffraction angle] is the vertical component of the wavenumber at different diffraction angles. Here, K is the ripple wavenumber along x axis, α_n is equivalent to $\pm nK/2$, and n is the number of diffraction angle; the summation is carried out up to $n = 8$, depending upon the angle of diffraction [$\theta_n = \sin^{-1}(\mp nK/k)$, where k is the operating wavenumber and K is already mentioned].

According to system transfer theory, in the frequency domain (Fig. 3), formation of the output $O(f)$ is a multiplication of source response $E(f)$ of the input at a direction θ with the response of the receiver system $F(f)$. In our present analysis, at normal incidence $\theta = 0°$, the array response is equivalent to having $F(f) = 1$, which leads to $O(f) = E(f)$. Source response, i.e., reflected pressure response $E(f)$ at $\theta = 0°$, is calculated from Eq. (5) by changing the operating frequency, to a range according to selected pulse length. The output response is then sampled and converted to the time domain by inverse Fourier transform (IFT) and plotted (Fig. 4) for different frequencies for sand, silt, and clay ripples. The normalized echo waveforms for pulse lengths of 2.12 and 4.2 ms are also presented. It is shown that the peak waveforms are maximum when the PDFs are Gaussian (Fig. 2) and slowly decaying toward a minimum when it is Rayleigh distributed for both pulse lengths. The sharpest peak is obtained at 4 kHz for sand ripples, for which the rms roughness is also the lowest.

Use of short pulses for high-resolution sonar systems is well known.[10] An echo waveform study was carried out at two different pulse lengths (2.12 and 4.2 ms) and observations show that the sidelobes are extended in time and higher echo peaks are obtained for the shorter pulse length (2.12 ms). The decayed echo may be an acausal effect generated due to the plane-wave reflection from ripple bottom boundary by sonar.[11] But unlike the 2.12-ms data, the peak return from silt ripples is higher than that for clay ripples for the 4.2-ms pulse length. The relative energy density output of the reflected echo waveforms are presented in Table III. The relative energy density was calculated form echo patterns of different bottom types by using the following expression:

$$E = \frac{1}{\rho c}\int_0^\infty p^2\,dt, \tag{6}$$

where ρc (1.5×10^5 g/cm^2 s) is the specific acoustic resistance of the seawater and p is the echo from Fig. 4. A close look at the values reveals that the energy reflected is maximum for both pulse lengths at 4 kHz for sand ripples. Only slight variations in energy density are observed for clay and silt ripples at other frequencies like 12 and 20 kHz.

TABLE III. Energy calculated at different pulse lengths for various sediment type.

Sonar number	Sediment type	Frequency kHz	Calculated relative energy density 2.12 ms	4.2 ms
1	sand	4	0.335×10^{-9}	0.130×10^{-9}
		12	0.316×10^{-10}	0.123×10^{-10}
		20	0.980×10^{-11}	0.384×10^{-11}
2	clay	4	0.214×10^{-9}	0.208×10^{-10}
		12	0.444×10^{-11}	0.173×10^{-11}
		20	0.743×10^{-12}	0.289×10^{-12}
3	silt	4	0.869×10^{-10}	0.338×10^{-10}
		12	0.608×10^{-11}	0.238×10^{-11}
		20	0.599×10^{-12}	0.233×10^{-12}

II. CONCLUSIONS

An observation is made to determine the amount of interaction effect of circular beams on ripple bottoms of sand, silt, and clay at different operating frequencies. Analyses, including calculation of PDFs, echo waveforms (at pulse lengths of 2.12 and 4.2 ms), and energy densities reflected from the different ripple bottoms, clearly demonstrates that the scattering effect is more prominent at higher frequencies as well as greater rms roughness, i.e., ripple height. It is also clear that scattering and, hence, echo fluctuation are affected more dramatically by the roughness and sonar frequency than by the different beam widths transmitted by the coaxial circular array at various frequencies [e.g., fading effects are higher even at the narrow beam widths (5.3°) for 20 kHz].

ACKNOWLEDGMENTS

The authors would like to thank R. R. Nair for his encouragement during the work and also would like to acknowledge the encouragement of Dr. B. N. Desai, Director NIO. The useful suggestions from N. H. Hashimi, Dr. E. Desa, and Professor K. K. Dey are also acknowledged. Thanks are due to G. Menon and S. Alison for typing the manuscript. Author is thankful to reviewer for his useful suggestions to improve the work.

[1] B. Chakraborty, "Coaxial circular array: Study of farfield pattern and field frequency responses," J. Acoust. Soc. Am. **79**, 1161–1163 (1986).
[2] T. K. Stanton and C. S. Clay, "Sonar echo statistics as a remote sensing tool: volume and seafloor," IEEE J. Ocean Eng. **OE-11**, 79–96 (1986).
[3] A. D. Dunsiger, N. A. Cochrane, and W. J. Vetter, "Seabed characterization from broad band acoustics echosounding with scattering models," IEEE J. Ocean. Eng. **OE-6**, 94–107 (1981).
[4] T. K. Stanton, "Sonar estimates of seafloor microroughness," J. Acoust. Soc. Am. **75**, 809–818 (1984).
[5] J. N. Tjotta and S. Tjotta, "Theoretical study of penetration of highly directional acoustic beams into sediments," J. Acoust. Soc. Am. **69**, 998–1008 (1981).
[6] D. E. Bell and W. J. Porter, "Remote sediments classification potential of reflected acoustic signals," in *Physics of Sound in Marine Sediments*, edited by L. Hampton (Plenum, New York, 1974), pp. 319–335.
[7] C. W. Horton, Sr., "Review of reverberation, scattering, and echo structure," J. Acoust. Soc. Am. **51**, 1049–1061 (1971).
[8] S. O. Rice, "Mathematical analysis of random noise," in *Selected Papers on Noise and Stochastic Processes*, edited by N. Wax (Dover, New York, 1954), pp. 133–294.
[9] I. Tolstoy and C. S. Clay, *Ocean Acoustics: Theory and Experiment in Underwater Sound* (McGraw-Hill, New York, 1966), pp. 199–201.
[10] B. G. Bardsley and D. A. Chirstensen, "Beam patterns from pulsed ultrasonic transducers using linear system theory," J. Acoust. Soc. Am. **69**, 25–30 (1981).
[11] M. H. Brill, X. Zabel, and S. L. Adams, "Time spread of acoustic signals reflecting from a fixed rough boundary," J. Acoust. Soc. Am. **75**, 1062–1070 (1984).